JST: Smart Systems and Devices
Volume 32, Issue 3, September 2022, 044-051

Takagi-Sugeno Fuzzy Approach with Compressed Representation for Overhead Crane System

Nhu Toan Nguyen, Danh Huy Nguyen, Tung Lam Nguyen, Thi Van Anh Nguyen*
Hanoi University of Science and Technology, Hanoi, Vietnam
**Corresponding author email: anh.nguyenthivan1@hust.edu.vn*

Abstract

This paper proposes a Takagi-Sugeno (TS) fuzzy approach for 2-dimensional of freedom overhead crane. Since this system is underactuated with nonlinear mathematical dynamic model, the requirement of achieving accurate positioning while eliminating oscillation is a challenging issue. The nonlinear sector decomposition is taken into implementation which uses the nonlinear terms in the dynamic model as scheduling variables to transform the initial system to TS representation. However, the number of TS fuzzy rules is exponential in the number of nonlinear elements in the system, leading to the increase of computational expense. Therefore, the reduced complexity method is introduced to minimize the scheduling variables in TS system. In addition, the uncertain system's components are also taken into consideration to enhance the robust property of the system when working in practical environment. The controller is constructed based on parallel distributed compensation (PDC) approach while the linear matrix inequalities (LMIs) technique is employed to analyse the system's stability. The effectiveness of the proposed method is demonstrated through numeral simulations.

Keywords: Overhead crane, Takagi-Sugeno fuzzy system, parallel distributed compensation, linear matrix inequalities.

1. Introduction

Overhead crane is considered as one of the most crucial hoisting apparatuses in automotive industry. This equipment is normally used to lift and transport heavy cargoes in construction sites, harbours, manufacturing companies, etc. However, most of them are still manipulated manually, which make it difficult to acquire high accuracy in control due to the dependence of human when working in persistent time. Besides, overhead crane is a typical underactuated system with nonlinear components due to the oscillation of payload in transporting process. The requirement of achieving precise position control of trolley while supressing payload swing to guarantee the effectiveness and safety at workplace is pressing problem. Therefore, the existence of an effective automatic controller for overhead crane system is put in high demand.

Regarding control methods for overhead crane, input shaping is a widely used with open-loop technique [1, 2]. The primary idea behind is that it constructs the control input according to the system's natural frequency such that the payload's vibration is reduced. The advantages of this approach are the robust property to frequency modelling errors and the straightforward implementation on real-time system. However, they are normally associated with slow response and require extra measurement devices. In term of closed loop approaches, traditional methods including sliding mode control, backstepping, etc., are studied intensively [3-5]. In [3] a robust controller with the core is sliding mode technique is introduced which ensure the accuracy of trolley position and the elimination of swing and skew angles in finite time. Besides, the robustness towards parametric uncertainties and initial conditions are also improved. Zhang *et al* present an adaptive sliding mode control accompanied with a proportional derivative controller for 2D overhead crane [4]. While former guarantees the system's stability, the uncertainties and external noises are compensated by the latter, therefore, system's performance is enhanced. In [5], the distributed model of 2D overhead crane using Hamilton's principle is introduced , which employs backstepping controller to drive the system to desired path. On the other hand, advanced control methods are also taken into considerations. Model predictive control methods [6] are utilized to effectively handle the input and output constraints of the system. However, computational complexity issue makes these controllers challenging to be embedded in hardware system. Neural network-based approaches [7] are proposed to approximate system parameters and external disturbances. Data-driven based control method [8], reinforcement learning [9] are used data from closed-loop experiments and optimal methods to construct dynamics model and adaptive parameters.

ISSN: 2734-9373
https://doi.org/10.51316/jst.160.ssad.2022.32.3.6
Received: February 11, 2022; accepted: May 27, 2022

In recent years, Takagi-Sugeno (TS) fuzzy control methods have been applied extensively in different control objectives. TS approach presents the system by a convex combination of local linear models, which facilitates the controller design and stability analysis. Normally, the nonlinear sector decomposition is taken into implementation to transform the initial system model to TS representation. The parallel distributed compensation (PDC) scheme combined with linear matrix inequalities (LMIs) technique is then utilized in order to construct global controller and ensure system's stability. In [10] a TS fuzzy controller is studied to guarantee the H-infinity performance for tracking problem of a 2 DOF manipulators. Akka *et al* [11] express the kinematic model of mobile robot in TS form, then PDC with each local controller being linear quadratic regular (LQR) combined with fuzzy controller is constructed to make the robot track the desired trajectories while avoiding obstacles. In [12], the TS fuzzy is integrated with nonlinear MPC controller for speed control of electrical vehicle system with time-delay effect, where the MPC is applied to handle the system constraints and guarantee the stability under TS fuzzy representation.

Nevertheless, the main disadvantage of TS fuzzy technique is the explosion of fuzzy rules because of the huge number of nonlinear elements existing in system's model, which increase computational burden. Therefore, the TS fuzzy approach is normally chosen for simple systems with few degrees of freedom. In this work, we propose a reduced complexity TS fuzzy system for 2D overhead crane system, which can effectively decrease the number of fuzzy rules while maintaining tracking performance. Besides, some parametric uncertainties are also considered to enhance the robust property of the system when being applied in real system.

The rest of the paper is organized as follows: Section 2 construct the mathematical dynamic equation of 2D overhead crane. Next, Section 3 illustrates the TS fuzzy system and the method to diminish the number of fuzzy rules. Section 4 provides the control design procedure and analysis the system's stability. The simulation results with different scenarios are illustrated in Section 5. Section 6 presents some conclusion remarks.

2. System Modelling

The overhead crane model consists of three primary elements: a trolley, a payload, and a cable. In this work, we assume that the cable length is unchanged during transporting process. The control targets of this system are driving the trolley to reference position and simultaneously supressing the oscillation of payload generated by the acceleration or deceleration of trolley. Fig. 1 shows the structure of 2-DOF overhead crane.

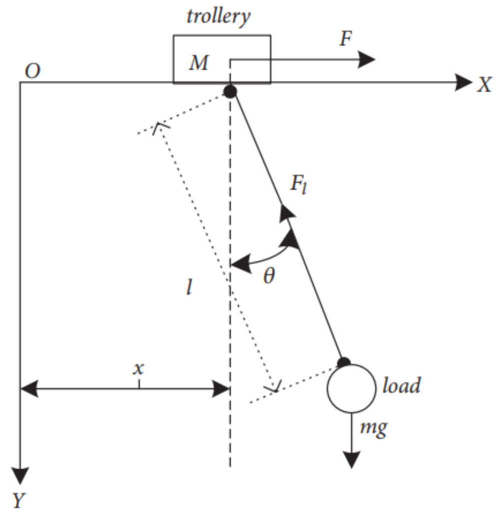

Fig. 1. 2-DOF overhead crane

The dynamic model of two-dimensional overhead crane with constant rope length is described as:

$$(M+m)\ddot{x}+ml\ddot{\theta}\cos\theta-ml\dot{\theta}^2\sin\theta+\mu\dot{x}=F \quad (1)$$

$$ml^2\ddot{\theta}+ml\ddot{x}\cos\theta+mgl\sin\theta=0 \quad (2)$$

where x is trolley's translational position, θ is oscillation angle of payload, F indicates translation force acting on trolley. l is rope's length, M and m are trolley's mass and payload's mass respectively, g is gravitation acceleration.

Define the state variables as $\mathbb{J}=\begin{bmatrix}x & \dot{x} & \theta & \dot{\theta}\end{bmatrix}^T$ $=\begin{bmatrix}\chi_1 & \chi_2 & \chi_3 & \chi_4\end{bmatrix}^T$, the mathematical model of overhead crane is rewritten as:

$$\begin{aligned}
\dot{\chi}_1 &= \chi_2\\
\dot{\chi}_2 &= \frac{mg\sin\chi_3\cos\chi_3+ml\chi_4^2\sin\chi_3-\mu\chi_2+F}{(M+m)-m\cos^2\chi_3}\\
\dot{\chi}_3 &= x_4\\
\dot{\chi}_4 &= \frac{(M+m)g\sin\chi_3+ml\chi_4^2\sin\chi_3\cos\chi_3}{\left[m\cos^2\chi_3-(M+m)\right]l}\\
&\quad+\frac{-\mu x_2\cos\chi_3+F\cos\chi_3}{\left[m\cos^2\chi_3-(M+m)\right]l}
\end{aligned} \quad (3)$$

The matrix form is

$$\begin{bmatrix}\dot{\chi}_1\\ \dot{\chi}_2\\ \dot{\chi}_3\\ \dot{\chi}_4\end{bmatrix}=\begin{bmatrix}0 & 1 & 0 & 0\\ 0 & a_{11} & a_{12} & a_{13}\\ 0 & 0 & 0 & 1\\ 0 & a_{21} & a_{22} & a_{23}\end{bmatrix}\begin{bmatrix}\chi_1\\ \chi_2\\ \chi_3\\ \chi_4\end{bmatrix}+\begin{pmatrix}0\\ b_1\\ 0\\ b_2\end{pmatrix}F \quad (4)$$
$$=\mathbf{M}\mathbb{J}+\mathbf{N}F$$

with

$$a_{11}=\frac{-\mu}{M+m\sin^2\chi_3}, a_{12}=\frac{mg\cos\chi_3\sin\chi_3}{M+m\sin^2\chi_3},$$

$$a_{13}=\frac{ml\chi_4\sin\chi_3}{M+m\sin^2\chi_3}, a_{21}=\frac{\mu\cos\chi_3}{l\left(M+m\sin^2\chi_3\right)},$$

$$a_{22}=\frac{-\left(M+m\right)g\sin\chi_3}{l\left(M+m\sin^2\chi_3\right)\chi_3}, a_{23}=\frac{-m\chi_4\sin\chi_3\cos\chi_3}{M+m\sin^2\chi_3},$$

$$b_1=\frac{1}{M+m\sin^2\chi_3}, b_2=\frac{-\cos\chi_3}{l\left(M+m\sin^2\chi_3\right)}.$$

3. Fuzzy System

3.1. TS Fuzzy Representation

For constructing TS fuzzy system, the sector nonlinearity method is normally employed in order to acquire accurate fuzzy description of nonlinear system in state space formulation.

Because of the physical limitations, the states vector J is bounded in the compact set $\mathbf{W}_{\mathrm{J}}$ defined as:

$$\mathbf{W}_{\mathrm{J}}=\left\{\mathrm{J}\in\mathbf{R}^{4\times 1} \mid \mathrm{J}_{\min}\le \mathrm{J}\le \mathrm{J}_{\max}\right\}.$$

Let $\varsigma_i, i=\overline{1,n}$ be the scheduling variables, which indicate the independent nonlinear term in matrices $\mathbf{M}$ and $\mathbf{N}$. Since $\mathrm{J}\in\mathbf{W}_{\mathrm{J}}$, the scheduling variables are also bounded, $\varsigma_i\in\left[\varsigma_{i\min},\varsigma_{i\max}\right], i=\overline{1,n}$ and can be equivalently represented as:

$$\varsigma_i=\tau_{\min}\left(\varsigma_i\right)\varsigma_{i\min}+\tau_{\max}\left(\varsigma_i\right)\varsigma_{i\max}$$

where

$$\tau_{\max}\left(\varsigma_i\right)=\frac{\varsigma_{i\max}-\varsigma_i}{\varsigma_{i\max}-\varsigma_{i\min}}$$
$$\tau_{\min}\left(\varsigma_i\right)=\frac{\varsigma_i-\varsigma_{i\min}}{\varsigma_{i\max}-\varsigma_{i\min}} \quad (5)$$

and satisfy:

$$\tau_{\max}\left(\varsigma_i\right)+\tau_{\min}\left(\varsigma_i\right)=1$$
$$\tau_{\max}\left(\varsigma_i\right)\ge 0, \tau_{\min}\left(\varsigma_i\right)\ge 0$$

The TS fuzzy system is represented as:

R^k : IF ς_1 is Λ_1^k and … and ς_n is Λ_n^k THEN

$$\dot{\mathrm{J}}=\mathbf{M}_k\mathrm{J}+\mathbf{N}_k\mathbf{F}, \quad k=1,2,...,h$$

where *h* and *n* are the number of fuzzy rules and input variables respectively. Hence, the original dynamic model can be described as follows:

$$\dot{\mathrm{J}}=\sum_{i=1}^{h}\tau_i\left(\varsigma\right)\left(\mathbf{M}_i\mathrm{J}+\mathbf{N}_i\mathbf{F}\right) \quad (6)$$

where $\tau_i\left(\varsigma\right)$ is the membership function of the i^{th} rules which is calculated as the product of the weighting functions corresponding to the fuzzy set in the rule:

$$\tau_i\left(\varsigma\right)=\prod_{j=1}^{n}\tau_{ij}\left(\varsigma_j\right), j=\overline{1,n} \quad (7)$$

with

$$\tau_{ij}\left(\varsigma_j\right)\in\left\{\tau_{\min}\left(\varsigma_j\right),\tau_{\max}\left(\varsigma_j\right)\right\}.$$

The matrices $\mathbf{M}_i,\mathbf{N}_i$ are formulated by replacing the components corresponding to the weighting functions applied in i^{th} fuzzy rule into matrices $\mathbf{M},\mathbf{N}$

However, the noticeable disadvantage of this approach is that the number of fuzzy rules is exponential in the number of nonlinearities. In practice, it could become intractable issues because of computation burden or algorithm limitations. Therefore, the number of rules should be considered carefully when design TS fuzzy system.

Regarding overhead crane model in (4), there are 4 nonlinear terms including

$$\varsigma_1=\frac{1}{M+m\sin^2 x_3},$$

$$\varsigma_2=\cos x_3,$$

$$\varsigma_3=\frac{\sin x_3}{x_3},$$

$$\varsigma_4=x_4\sin x_3$$

which requires $2^4=16$ fuzzy rules in total according to TS fuzzy model theory. Therefore, the approximation approach introduced in the next subsection is employed to minimize the quantity of fuzzy rules.

3.2. Approximation Mechanism

To minimize the complexity of the fuzzy system, the reduced complexity approach is used. Specifically, some nonlinear term in the matrices $\mathbf{M},\mathbf{N}$ are now considered as uncertain components instead of ingredients of scheduling variables. Here, $\varsigma_4=x_4\sin x_3$ is regarded as the uncertainty. Hence, the number of nonlinear terms used for scheduling variables is reduced to three, leading to the number of fuzzy rules decrease by a half to $2^3=8$. Specifically, the scheduling variable ς_4 is rewritten as follows:

$$\varsigma_4(t) = \varsigma_{4m} + \lambda(t)\varsigma_{4r} \tag{8}$$

with $\|\lambda\| \le 1$ and

$$\varsigma_{4m} = \frac{1}{2}\left(\varsigma_{4\max} + \varsigma_{4\min}\right)$$

$$\varsigma_{4r} = \frac{1}{2}\left(\varsigma_{4\max} - \varsigma_{4\min}\right)$$

Besides, since the value of trolley mass and cable length are varied in practical use, they are also unknown elements. Hence, the system model with uncertainties is represented as follows:

$$\dot{\mathrm{J}} = \sum_{k=1}^{h} \tau_k(\varsigma)\left(\tilde{\mathbf{M}}_k \mathrm{J} + \tilde{\mathbf{N}}_k \mathbf{F}\right) \tag{9}$$

where $\tilde{\mathbf{M}}_k = \mathbf{M}_k + \Delta\mathbf{M}_k, \tilde{\mathbf{N}}_k = \mathbf{N}_k + \Delta\tilde{\mathbf{N}}_k$. The system uncertainties are of the forms:

$$\begin{aligned} \Delta\mathbf{M}_i &= \Gamma_m^T \Omega_m \mathrm{i}_{mi} \\ \Delta\mathbf{N}_i &= \Gamma_n^T \Omega_n \mathrm{i}_{ni} \end{aligned} \tag{10}$$

with

$$\|\mathbf{\Omega}_{mi}\| \le \mathbf{I} \text{ and } \|\mathbf{\Omega}_{ni}\| \le \mathbf{I} \tag{11}$$

The membership functions for TS system are illustrated in Fig. 2. which are presented as "big", "small" and can be calculated as in (5).

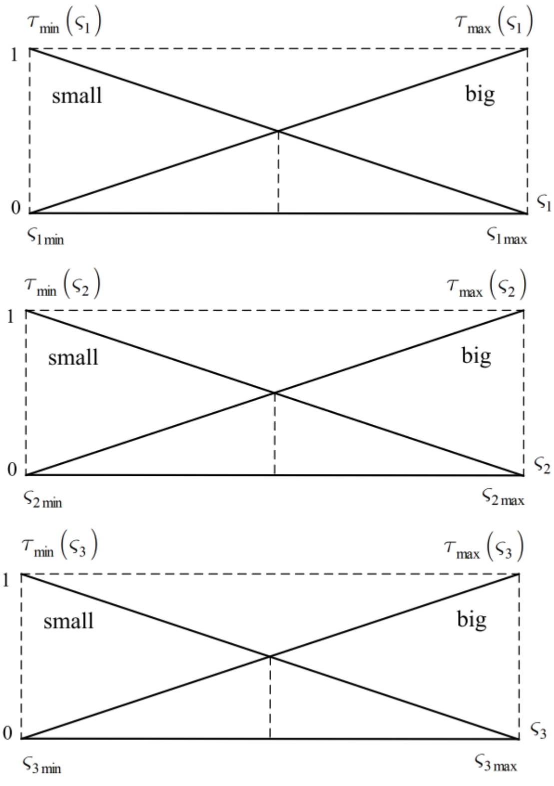

Fig. 2. Membership functions

And the scheduling variables includes:

$$\varsigma_1 = \frac{1}{M + m\sin^2 x_3} = \tau_{\max}(\varsigma_1)\varsigma_{1\max} + \tau_{\min}(\varsigma_1)\varsigma_{1\min}$$

$$\varsigma_2 = \cos x_3 = \tau_{\max}(\varsigma_2)\varsigma_{2\max} + \tau_{\min}(\varsigma_2)\varsigma_{2\min}$$

$$\varsigma_3 = \frac{\sin x_3}{x_3} = \tau_{\max}(\varsigma_3)\varsigma_{3\max} + \tau_{\min}(\varsigma_3)\varsigma_{3\min}$$

where the value of $\varsigma_{1\max}, \varsigma_{1\min}, \varsigma_{2\max}, \varsigma_{2\min}, \varsigma_{3\max}, \varsigma_{3\min}$ are determined in Section 5.

4. Control Design

To construct controller and analyse stability condition for TS systems (9), the LMIs approach is employed.

Lemma 1 *(Young's relation [13]):* Given constant matrices **X** and matrices **Y** of appropriate dimensions for $\sigma > 0$, the following inequality holds:

$$\mathbf{X}^T\mathbf{Y} + \mathbf{Y}^T\mathbf{X} \le \sigma\mathbf{X}^T\mathbf{X} + \frac{1}{\sigma}\mathbf{Y}^T\mathbf{Y}$$

Theorem 1: If there exist a positive definite matrix $\mathbf{\Xi}$, matrices $\mathrm{C}_i, i = 1,...,h$, and scalars $\lambda_m > 0$ and $\lambda_n > 0$ satisfying inequalities

$$\Psi_{ii} < 0 \tag{12}$$

$$\Psi_{ij} < 0,\ i < j \text{ w.r.t } \rho_i \cap \rho_j = \varnothing \tag{13}$$

where

$$\Psi_{ij} = \begin{bmatrix} \mathbf{Z}_{ij} + \lambda_m \Gamma_m \Gamma_m^T + \lambda_n \Gamma_n \Gamma_n^T & \mathrm{X}\mathrm{i}_{mi}^T & -\mathrm{C}_j^T \mathrm{i}_{ni}^T \\ \mathrm{i}_{mi}\mathrm{X} & -\lambda_m \mathrm{I} & 0 \\ -\mathrm{i}_{ni}\mathrm{C}_j & 0 & -\lambda_n \mathrm{I} \end{bmatrix} \tag{14}$$

with

$$\mathrm{Z}_{ij} = \mathbf{M}_i\mathbf{X} - \mathbf{N}_i\mathrm{C}_j + \mathbf{X}^T\mathbf{M}_i - \mathrm{C}_j^T\mathbf{N}_i^T$$

the TS fuzzy system (9) with parallel distributed compensation (PDC) controller of following form:

$$\mathbf{F} = -\sum_{i=1}^{h} \tau_i(\varsigma)\mathrm{K}_i \mathrm{J} \tag{15}$$

with $\mathbf{K}_i = \mathrm{C}_i\mathbf{X}^{-1}, \mathbf{\Xi} = \mathbf{X}^{-1}$, is global asymptotic stable.

Proof:

Consider the Lyapunov function:

$$V = \mathrm{J}^T \mathbf{\Xi} \mathrm{J} \tag{16}$$

Its derivative is:

$$\begin{aligned} \dot{V} &= \dot{\mathrm{J}}^T \mathbf{\Xi} \mathrm{J} + \mathrm{J}^T \mathbf{\Xi} \dot{\mathrm{J}} \\ &= \left(\sum_{i=1}^{h} \tau_i(\varsigma)\left(\tilde{\mathbf{M}}_i \mathrm{J} + \tilde{\mathbf{N}}_i \mathbf{F}\right)\right)^T \mathbf{\Xi}\mathrm{J} \\ &\quad + \mathrm{J}^T \mathbf{\Xi} \sum_{i=1}^{h} \tau_i(\varsigma)\left(\tilde{\mathbf{M}}_i \mathrm{J} + \tilde{\mathbf{N}}_i \mathbf{F}\right) \end{aligned} \tag{17}$$

Substitute controller (15) into (17) yields:

$$\begin{aligned}\dot{V} &= \left(\sum_{i=1}^{h}\tau_i(\varsigma)\left(\tilde{\mathbf{M}}_i - \sum_{i=1}^{h}\tau(\varsigma)\tilde{\mathbf{N}}_i\mathrm{K}_i\right)\mathrm{J}\right)^T \mathbf{\Xi}\mathrm{J} \\ &+ \mathrm{J}^T\mathbf{\Xi}\left(\sum_{i=1}^{h}\tau_i(\varsigma)\left(\tilde{\mathbf{M}}_i - \sum_{i=1}^{h}\tau(\varsigma)\tilde{\mathbf{N}}_i\mathrm{K}_i\right)\mathrm{J}\right) \\ &= \mathrm{J}^T\sum_{i=1}^{h}\sum_{j=1}^{h}\tau_i(\varsigma)\tau_j(\varsigma)\mathbf{\Xi}\left(\tilde{\mathbf{M}}_i - \tilde{\mathbf{N}}_i\mathrm{K}_j\right)\mathrm{J} \\ &+ \mathrm{J}\sum_{i=1}^{h}\sum_{j=1}^{h}\tau_i(\varsigma)\tau_j(\varsigma)\mathbf{\Xi}\left(\tilde{\mathbf{M}}_i - \tilde{\mathbf{N}}_i\mathrm{K}_j\right)\mathrm{J}^T \qquad (18) \\ &= \mathrm{J}^T\sum_{i=1}^{h}\sum_{j=1}^{h}\tau_i(\varsigma)\tau_j(\varsigma)\mathbf{\Xi}\big(\mathbf{M}_i - \mathbf{N}_i\mathrm{K}_j \\ &+ \Delta\mathbf{M}_i - \Delta\mathbf{N}_i\mathrm{K}_j\big)\mathrm{J} + \mathrm{J}\sum_{i=1}^{h}\sum_{j=1}^{h}\tau_i(\varsigma)\tau_j(\varsigma) \\ &\times\mathbf{\Xi}\left(\mathbf{M}_i - \mathbf{N}_i\mathrm{K}_j + \Delta\mathbf{M}_i - \Delta\mathbf{N}_i\mathrm{K}_j\right)\vartheta^T\end{aligned}$$

Hence, $\dot{V} < 0$ if and only if:

$$\begin{aligned}&\sum_{i=1}^{h}\sum_{j=1}^{h}\tau_i(\varsigma)\tau_j(\varsigma)\mathbf{\Xi}\left(\left(\mathbf{M}_i - \mathbf{N}_i\mathrm{K}_j\right)\right. \\ &+\sum_{i=1}^{h}\sum_{j=1}^{h}\tau_i(\varsigma)\tau_j(\varsigma)\mathbf{\Xi}\left(\Delta\mathbf{M}_i - \Delta\mathbf{N}_i\mathrm{K}_j\right) \qquad (19) \\ &+\sum_{i=1}^{h}\sum_{j=1}^{h}\tau_i(\varsigma)\tau_j(\varsigma)\left(\left(\mathbf{M}_i - \mathbf{N}_i\mathrm{K}_j\right)^T\mathbf{\Xi}^T\right. \\ &+\sum_{i=1}^{h}\sum_{j=1}^{h}\tau_i(\varsigma)\tau_j(\varsigma)\left(\Delta\mathbf{M}_i - \Delta\mathbf{N}_i\mathrm{K}_j\right)^T\mathbf{\Xi}^T \\ &< 0\end{aligned}$$

Let $\mathbf{K}_i = \mathrm{C}_i\mathbf{X}^{-1}, \mathbf{\Xi} = \mathbf{X}^{-1}$, (19) is rewritten as:

$$\begin{aligned}&\sum_{i=1}^{h}\sum_{j=1}^{h}\tau_i(\varsigma)\tau_j(\varsigma)\left(\mathbf{M}_i\mathbf{X} - \mathbf{N}_i\mathrm{C}_j + \Delta\mathbf{M}_i - \Delta\mathbf{N}_i\mathrm{C}_j\right) \\ &+\sum_{i=1}^{h}\sum_{j=1}^{h}\tau_i(\varsigma)\tau_j(\varsigma)\left(\mathbf{M}_i\mathbf{X} - \mathbf{N}_i\mathrm{C}_j + \Delta\mathbf{M}_i - \Delta\mathbf{N}_i\mathrm{C}_j\right)^T \\ &< 0\end{aligned} \qquad (20)$$

From (10) and **Lemma 1**, we have:

$$\begin{aligned}&\sum_{i=1}^{h}\sum_{j=1}^{h}\tau_i(\varsigma)\tau_j(\varsigma)\Big(\Delta\mathbf{M}_i\mathbf{X} - \Delta\mathbf{N}_i\mathrm{C}_j \\ &\qquad + \left(\Delta\mathbf{M}_i\mathbf{X} - \Delta\mathbf{N}_i\mathrm{C}_j\right)^T\Big) \\ &= \sum_{i=1}^{h}\sum_{j=1}^{h}\tau_i(\varsigma)\tau_j(\varsigma)\left(\Gamma_m \quad \Gamma_n\right) \\ &\qquad \times\begin{pmatrix}\Omega_m & 0 \\ 0 & \Omega_n\end{pmatrix}\begin{pmatrix}{}_{mi}\mathbf{X} \\ -{}_{ni}\mathrm{C}_j\end{pmatrix} \\ &+\sum_{i=1}^{h}\sum_{j=1}^{h}\tau_i(\varsigma)\tau_j(\varsigma)\left(\mathbf{X}_{mi}^T \quad -\mathrm{C}_j{}_{ni}^T\right) \\ &\qquad \times\begin{pmatrix}\Omega_m^T & 0 \\ 0 & \Omega_n^T\end{pmatrix}\begin{pmatrix}\Gamma_m^T \\ \Gamma_n^T\end{pmatrix} \\ &\le \sum_{i=1}^{h}\sum_{j=1}^{h}\tau_i(\varsigma)\tau_j(\varsigma)\left(\mathbf{X}_{mi}^T \quad -\mathrm{C}_j{}_{ni}^T\right)\Lambda^{-1} \\ &\quad \times\sum_{i=1}^{h}\sum_{j=1}^{h}\tau_i(\varsigma)\tau_j(\varsigma)\begin{pmatrix}{}_{mi}\mathbf{X} \\ -{}_{ni}\mathrm{C}_j\end{pmatrix} \\ &\quad + \left(\Gamma_m \quad \Gamma_n\right)\Lambda\begin{pmatrix}\Gamma_m^T \\ \Gamma_n^T\end{pmatrix}\end{aligned} \qquad (21)$$

with

$$\Lambda = \begin{pmatrix}\lambda_m\mathbf{I} & \mathbf{0} \\ \mathbf{0} & \lambda_n\mathbf{I}\end{pmatrix}, \lambda_m > 0, \lambda_n > 0 \qquad (21)$$

Therefore, (20) can be further written as:

$$\begin{aligned}&\sum_{i=1}^{h}\sum_{j=1}^{h}\tau_i(\varsigma)\tau_j(\varsigma)\Big(\mathbf{M}_i\mathbf{X} - \mathbf{N}_i\mathrm{C}_j \\ &\qquad + \left(\mathbf{M}_i\mathbf{X} - \mathbf{N}_i\mathrm{C}_j\right)^T\Big) \qquad (22) \\ &+\sum_{i=1}^{h}\sum_{j=1}^{h}\tau_i(\varsigma)\tau_j(\varsigma)\left(\mathbf{X}\mathrm{i}_{mi}^T \quad -\mathrm{C}_j\mathrm{i}_{ni}^T\right)\Lambda^{-1} \\ &\times\sum_{i=1}^{h}\sum_{j=1}^{h}\tau_i(\varsigma)\tau_j(\varsigma)\begin{pmatrix}\mathrm{i}_{mi}\mathbf{X} \\ -\mathrm{i}_{ni}\mathrm{C}_j\end{pmatrix} \\ &+\left(\Gamma_m \quad \Gamma_n\right)\Lambda\begin{pmatrix}\Gamma_m^T \\ \Gamma_n^T\end{pmatrix} < 0\end{aligned}$$

Using Schur complement yields:

$$\begin{bmatrix}\mathrm{Z}_{ij} + \lambda_m\Gamma_m\Gamma_m^T + \lambda_n\Gamma_n\Gamma_n^T & \mathrm{X}\mathrm{i}_{mi}^T & -\mathrm{C}_j^T\mathrm{i}_{ni}^T \\ \mathrm{i}_{mi}\mathrm{X} & -\lambda_m\mathrm{I} & 0 \\ -\mathrm{i}_{ni}\mathrm{C}_j & 0 & -\lambda_n\mathrm{I}\end{bmatrix} < 0 \qquad (23)$$

with

$$\mathrm{Z}_{ij} = \mathbf{M}_i\mathbf{X} - \mathbf{N}_i\mathrm{C}_j + \mathbf{X}^T\mathbf{M}_i - \mathrm{C}_j^T\mathbf{N}_i^T$$

The proof is completed.

Remark 1: The system response's speed is related to the largest Lyapunov exponent, called decay rate. Hence, the decay rate $\alpha > 0$ is added to (12) and (13) to obtain property $\dot{V} \le -2\alpha V$. Then, the matrices $\mathbf{\Xi}$, $\mathrm{C}_i, i = \overline{1,h}$, and decay rate α are acquired by solving the LMIs issue:

$$\underset{\mathbf{X},\mathbf{M}_1,\dots,\mathbf{M}_h}{\text{maximize}}\ \alpha$$

subject to

$$\begin{bmatrix}\bar{\mathrm{Z}}_{ij} + \lambda_m\Gamma_m\Gamma_m^T + \lambda_n\Gamma_n\Gamma_n^T & \mathrm{X}\mathrm{i}_{mi}^T & -\mathrm{C}_j^T\mathrm{i}_{ni}^T \\ \mathrm{i}_{mi}\mathrm{X} & -\lambda_m\mathrm{I} & 0 \\ -\mathrm{i}_{ni}\mathrm{C}_j & 0 & -\lambda_n\mathrm{I}\end{bmatrix} < 0 \quad (24)$$

with

$$\bar{\mathrm{Z}}_{ij} = \mathbf{M}_i\mathbf{X} - \mathbf{N}_i\mathrm{C}_j + \mathbf{X}^T\mathbf{M}_i - \mathrm{C}_j^T\mathbf{N}_i^T + 2\alpha\mathbf{X}$$

Remark 2: Once the stability condition is transformed into the LMI condition, the efficient convex optimization algorithms can be employed to solve the problem precisely. There exist many efficient numerical optimizers to solve the LMI problem such as LMILAB, SeDuMi, SDPT3, VSDP, or LMIRank, which are also available in many toolboxs such as Matlab® LMI toolbox, Sedumi, or Yalmip.

5. Simulation results

This section carries out some simulation tests to express the validity of designed controller. The parameters of system's model are opted as follows:

$$\begin{aligned} M &= 10\,kg \\ m &= 5\,kg, \\ l &= 1\,m, \\ g &= 9.8\,m/s^2, \\ \mu &= 0.3. \end{aligned} \tag{25}$$

The system works under some limitations:

$$\begin{aligned} |x| &\le 3\ m, \qquad |\theta| \le \frac{\pi}{12}rad \\ |\dot{x}| &\le 5\ m/s, \qquad |\dot{\theta}| \le \frac{\pi}{4}rad/s \end{aligned} \tag{26}$$

From the boundary conditions of state variables and the system parameters, the limitations of scheduling variables are acquired as follows:

$$\begin{aligned} \varsigma_{1\min} &= 0.0968, \qquad \varsigma_{1\max} = 0.1, \\ \varsigma_{2\min} &= 0.9659, \qquad \varsigma_{2\max} = 1.0, \\ \varsigma_{3\min} &= 0.9886, \qquad \varsigma_{3\max} = 1.0, \end{aligned} \tag{27}$$

The control gains are obtained by solving the LMI conditions (25). In this paper, the SeDuMi solver within the Yalmip toolbox is used, resulting in the control gains as follows:

$\mathbf{K}_1$ = 1.0e+2×
[0.4215 1.0328 -5.7327 -1.0042];
$\mathbf{K}_2$ = 1.0e+2×
[0.4222 1.0347 -5.7552 -1.0038];
$\mathbf{K}_3$ = 1.0e+2×
[0.4265 1.0433 -5.8163 -1.0267];
$\mathbf{K}_4$ = 1.0e+2×
[0.4268 1.0442 -5.8320 -1.0253];
$\mathbf{K}_5$ = 1.0e+2×
[0.4216 1.0330 -5.7339 -1.0044];
$\mathbf{K}_6$ = 1.0e+2×
[0.4222 1.0349 -5.7561 -1.0038];
$\mathbf{K}_7$ = 1.0e+2×
[0.4263 1.04282 -5.8133 -1.0263];
$\mathbf{K}_8$ = 1.0e+2×
[0.4268 1.0442 -5.8323 -1.0253];

There reference position for trolley is set to $x_d = 0.5\ m$ in first 15 second, then it changes to $x_d = 1\ m$ in next 15 second before plummeting to $0.3\,m$ at the end of simulation period.

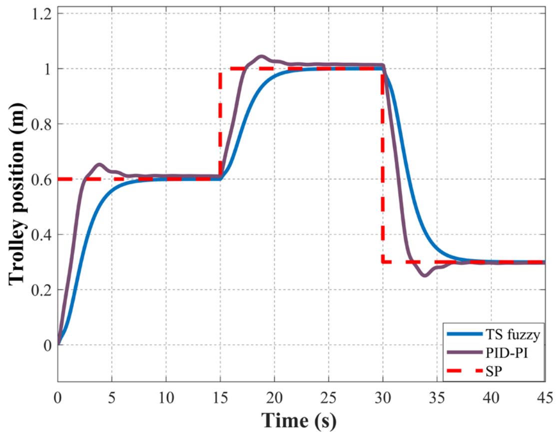

Fig. 3. Trolley position (m)

To illustrate the validity of the proposed method, two cases of study are implemented as follows:

Case study I

The PID-PI controller is implemented to make the comparison with the proposed method, in which the outer-loop PID controller is responsible for driving the trolley to the desired position while the inner-loop PI controller stabilizes the trolley's velocity and eliminates the payload swing. The control gains for PID-PI controller are obtained by experiments with following parameters:

PID: $K_P = 2;\ K_D = 1.5;\ \ K_I = 0.01$,

PI: $K_P = 9.46;\ \ K_I = 0.282$.

Fig. 3 and 4 illustrate the trajectories of trolley and payload under proposed TS controller and the PID-PI controller when all the parameters are exactly known. The red dash line denotes the setpoint while the blue line and purple line indicate the response of the system using the TS fuzzy controller and PID-PI controller respectively. It is apparent that the PID-PI controller requires higher time convergence and has overshoots when the setpoint changes its value. In addition, the payload is oscillated greatly within 0.08 rad before gradually decrease to zero. On the other hand, the TS fuzzy controller can manoeuvrer the trolley to reference position in less than 7 seconds while keep the swing angle less than 0.03 rad. Therefore, the results show that the proposed controller can drive the system to track the desired position rapidly while eliminate the payload swing.

Fig. 5 shows the translation force acting on the trolley of both comparing methods. There are the sharp changes of control input when the set point changes its value, but this phenomenon can be alleviated by designing a smoother reference trajectory.

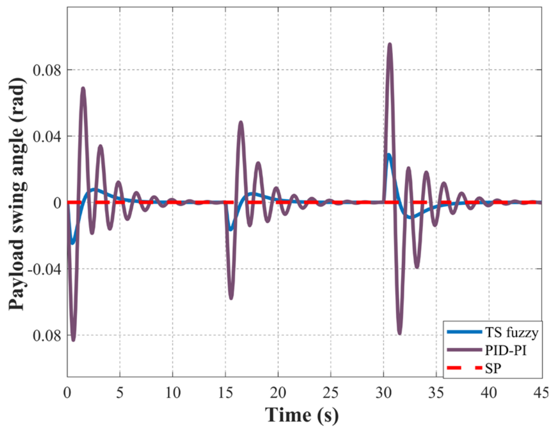

Fig. 4. Payload swing angle (rad)

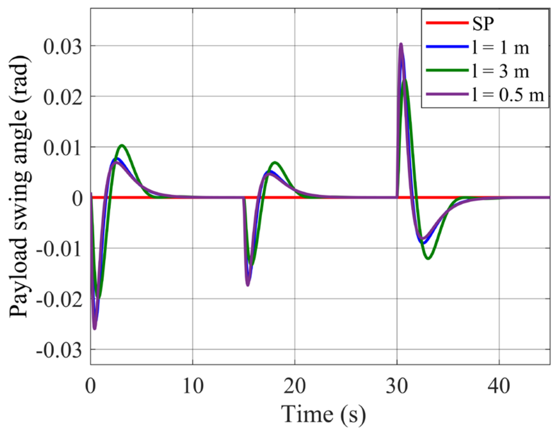

Fig. 5. Payload swing angle with variations of cable length

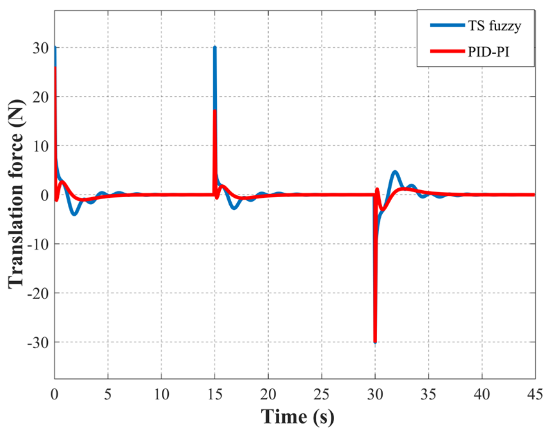

Fig. 6 Control input

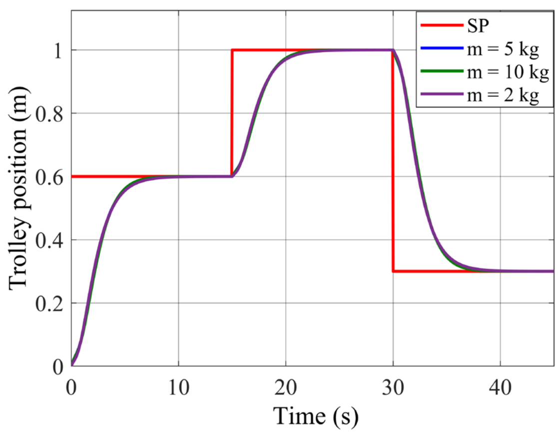

Fig. 7. Trolley position with variations of payload mass

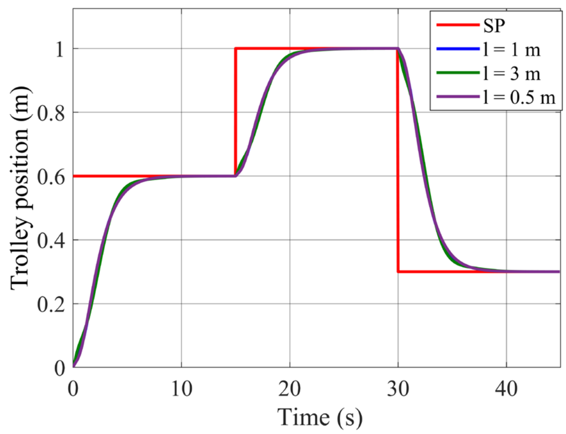

Fig. 8. Trolley position with variations of cable length

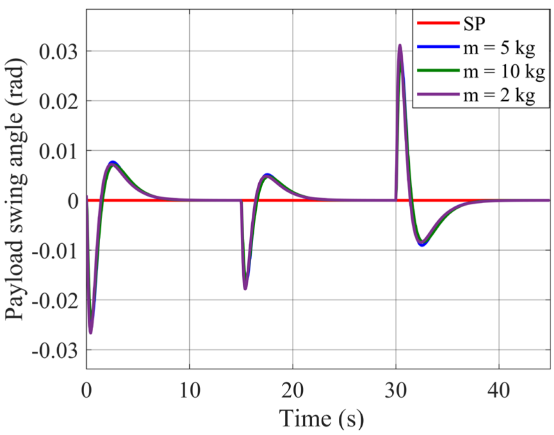

Fig. 9. Payload swing angle with variations of payload mass

Case study II

In practice, the rope's length and payload's mass are two varied parameters. Hence, to demonstrate the control method's robustness in occurrence of ambiguous components, in this case study, two additional tests considering the variation of rope's length and payload's mass are taken into implementation. Firstly, the value of cable length is altered from $1m$ to $3m$ and $0.5m$ respectively. Fig. 6 and Fig. 7 depict the outcome for these cases. The performance of the system is still maintained regardless of the change of cable length. Secondly, the payload mass is varied to $10\,kg$ and $2\,kg$ respectively. According to Fig. 8 and 9, the similar pattern is obtained in three cases, which highlights the robustness of this method.

6. Conclusion

In this work, TS fuzzy system is introduced to control the 2-DOF overhead crane system. The explosion of fuzzy rules problem is solved by the approximation method. Besides, the uncertain elements are considered to improve the robustness of the system when working in practical applications. The controller is designed based one PDC scheme while LMIs technique is employed to analyse system's stability. The numerical results illustrate the validity of this approach.

Acknowledgments

This research is funded by Hanoi University of Science and Technology (HUST) under project number T2021-TT-002.

References

[1] L. Ramli, Z. Mohamed, M. Efe, I. M. Lazim, H. Jaafar, Efficient swing control of an overhead crane with simultaneous payload hoisting and external disturbances, Mechanical Systems and Signal Processing, vol. 135, p. 106326, 2020. https://doi.org/10.1016/j.ymssp.2019.106326

[2] M. J. Maghsoudi, Z. Mohamed, S. Sudin, S. Buyamin, H. Jaafar, and S. Ahmad, An improved input shaping design for an efficient sway control of a nonlinear 3D overhead crane with friction, Mechanical Systems and Signal Processing, vol. 92, pp. 364-378, 2017. https://doi.org/10.1016/j.ymssp.2017.01.036

[3] D. Chwa, Sliding-mode-control-based robust finite-time antisway tracking control of 3-D overhead cranes, IEEE Transactions on Industrial Electronics, vol. 64, no. 8, pp. 6775-6784, 2017. https://doi.org/10.1109/TIE.2017.2701760

[4] M. Zhang *et al.*, Adaptive proportional-derivative sliding mode control law with improved transient performance for underactuated overhead crane systems, IEEE/CAA Journal of Automatica Sinica, vol. 5, no. 3, pp. 683-690, 2018. https://doi.org/10.1109/JAS.2018.7511072

[5] T. Nguyen, M. Duong, and T. Do, A direct Lyapunov-backstepping approach for stabilizing gantry systems with flexible cable, Proceedings of Engineering and Technology Innovation, vol. 8, p. 15, 2018.

[6] G. Galuppini, L. Magni, and D. M. Raimondo, Model predictive control of systems with deadzone and saturation, Control Engineering Practice, vol. 78, pp. 56-64, 2018. https://doi.org/10.1016/j.conengprac.2018.06.010

[7] H. M. Cuong, P. Van Trieu, L. C. Nho, and V. D. Thuan, Adaptive neural network sliding mode control of shipboard container cranes considering actuator backlash, Mechanical Systems and Signal processing, vol. 112, pp. 233-250, 2018. https://doi.org/10.1016/j.ymssp.2018.04.030

[8] N. S. A. Shukor and M. A. Ahmad, Data-driven PID tuning based on safe experimentation dynamics for control of double-pendulum-type overhead crane, in Intelligent Manufacturing & Mechatronics, Springer, 2018, pp. 295-303. https://doi.org/10.1007/978-981-10-8788-2_27

[9] X. Sun and Z. Xie, Reinforcement Learning-Based Backstepping Control for Container Cranes, Mathematical Problems in Engineering, vol. 2020, 2020. https://doi.org/10.1155/2020/2548319

[10] V.-A. Nguyen, A.-T. Nguyen, A. Dequidt, L. Vermeiren, and M. Dambrine, LMI-based 2-DoF control design of a manipulator via TS descriptor approach, IFAC-PapersOnLine, vol. 51, no. 22, pp. 102-107, 2018. https://doi.org/10.1016/j.ifacol.2018.11.525

[11] K. Akka and F. Khaber, Optimal fuzzy tracking control with obstacles avoidance for a mobile robot based on Takagi-Sugeno fuzzy model, Transactions of the Institute of Measurement and Control, vol. 41, no. 10, pp. 2772-2781, 2019. https://doi.org/10.1177/0142331218811462

[12] M. H. Khooban, N. Vafamand, T. Niknam, T. Dragicevic, and F. Blaabjerg, Model-predictive control based on Takagi-Sugeno fuzzy model for electrical vehicles delayed model, IET Electric Power Applications, vol. 11, no. 5, pp. 918-934, 2017. https://doi.org/10.1049/iet-epa.2016.0508

[13] A. Zemouche, R. Rajamani, B. Boulkroune, H. Rafaralahy, and M. Zasadzinski, H∞ circle criterion observer design for Lipschitz nonlinear systems with enhanced LMI conditions, in 2016 American Control Conference (ACC), 2016, pp. 131-136: IEEE. https://doi.org/10.1109/ACC.2016.7524904